Inorganic Chemistry

pubs.acs.org/IC Article

Mono- and Bis-Phosphine Promoted Incorporation of Boron, Nitrogen, and Phosphorus into Heterocycles via Staudinger Reactions of Borafluorene Azides

Bi Youan E. Tra, Andrew Molino, Kimberly K. Hollister, Samir Kumar Sarkar, Diane A. Dickie, David J. D. Wilson,* and Robert J. Gilliard, Jr*



Cite This: Inorg. Chem. 2024, 63, 11604-11615



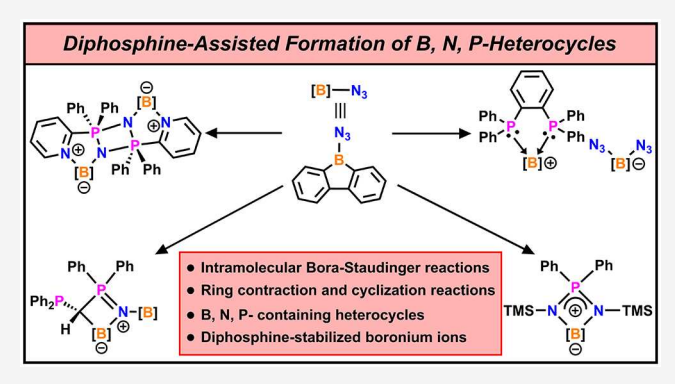
ACCESS

III Metrics & More

Article Recommendations

s Supporting Information

ABSTRACT: We report the synthesis and characterization of a series of BNP-incorporated borafluorenate heterocycles formed via thermolysis reactions of pyridylphosphine and bis(phosphine)-coordinated borafluorene azides. The use of diphenyl-2-pyridylphosphine (PyPh₂P), trans-1,2-bis(diphenylphosphino)ethylene (Ph₂P(H)C=C(H)PPh₂), and bis(diphenylphosphino)methane (Ph₂PC(H₂)PPh₂) as stabilizing ligands resulted in Staudinger reactions to form complex heterocycles with four- (BN₂P, BNPC, P₂N₂) and five-membered (BNP₂C and BN₂PC) rings, which were successfully isolated and fully characterized by multinuclear NMR and X-ray crystallography. However, when bis(diphenylphosphino)benzene (Ph₂P-Ph-PPh₂) was used as the ligand in a reaction with 9-bromo-9-borafluorene (BF-Br), due to the close



proximity of the donor P atoms, the diphosphine-stabilized borafluoronium ion with an unusual borafluorene dibromide anion was formed. Reaction of the borafluoronium ion with trimethylsilyl azide left the cation intact, and the dibromide anion was substituted by a diazide. Density functional theory calculations were used to provide mechanistic insight into the formation of these new boracyclic compounds. This work highlights a new method in which donor phosphine ligands may be used to promote dimerization, cyclization, and ring contraction reactions to produce boracycles via Staudinger reactions.

■ INTRODUCTION

9-Borafluorenes are a popular class of boron-centered polycyclic molecules which feature a central 5-membered boron-containing heterocycle with a phenyl ring fused to each side. 1-6 In recent years, there have been a substantial number of key advances toward their fundamental reaction chemistry, ^{7–14} optical properties, ^{15–19} and use as chemical synthons for more complex molecules. ^{3,20–37} While investigations of tricoordinate borafluorenes are well-established,³⁸ less is known regarding the reactivity of tetracoordinate borafluorene compounds despite the fact that a significant number of suitable precursors exist. Our laboratory has used carbenecoordinated borafluorene halides to access rare examples of cationic ^{39,40} and anionic borafluorenes, ^{41–45} as well as stable radicals⁴⁶ with spin density delocalized throughout the polycyclic aromatic hydrocarbon (PAH) framework.⁴⁷ More recently, we synthesized a series of mono(phosphine)coordinated borafluorene azides which, under thermal or photochemical conditions, afforded an array of compounds containing 4-membered B₂N₂ rings with an exocyclic phosphinimine moiety (Figure 1A).⁴⁸ While organic azides participating in Staudinger ligation reactions are wellestablished, examples of phosphine-promoted N₂ loss at

boron are rare.^{50–53} The chemistry depicted in Figure 1A represents an unusual example in which an intramolecular Staudinger reaction has been used to produce boracycles. We hypothesized that using a linker which has two L-type donors (Lewis base) that are available to bind tricoordinate borafluorenes (Lewis acid) may serve as a simple method to obtain extended bis(borafluorene) precursors en route to new B and BNP heterocycles. Thus far, strategies to incorporate multiple borafluorene moieties in a single molecule have involved prelinking borafluorenes through fusion or via direct bonding at the boron center.^{1,27,54–57} The use of multiple coordination reactions to prepare borafluorene precursors provides a new strategy that requires minimal synthetic demand.

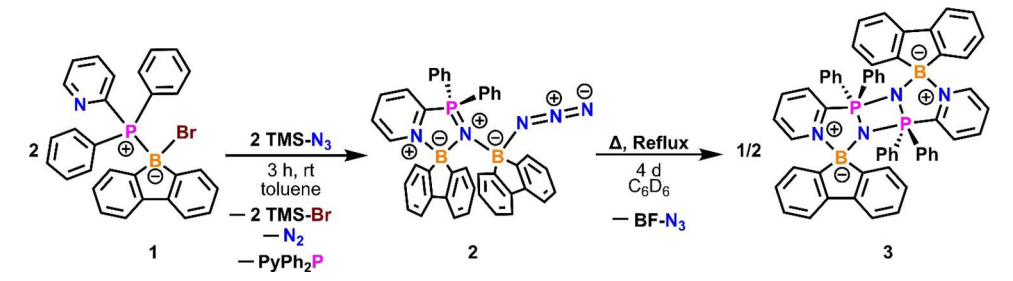
Received: February 29, 2024
Revised: May 12, 2024
Accepted: May 28, 2024
Published: June 12, 2024





Figure 1. (A) Synthesis of BN-borafluorenate heterocycles with an exocyclic phosphinimine moiety. (B) Synthesis of BNP-borafluorenate heterocycles with an endocyclic phosphinimine moiety; synthesis of boronium ion $[(Ph_2P-Ph-PPh_2)-(BF)][(BF)-X_2]$ X = Br, N₃; BF = borafluorene (this work).

Scheme 1. Synthesis of (Pyridyl)(diphenyl)phosphine-borafluorene-bromide Adduct 1, 5-Membered BN₂PC Ring-Containing Bis(borafluorene) Complex 2 and BN₂PC and P₂N₂ Ring-Containing Bis(borafluorene) 3^a



^aBF-N₃ = 9-azido-9-borafluorene; TMS = trimethylsilyl; Py = pyridyl.

Herein, we disclose the synthesis, molecular structures, and computational analysis of boron-, nitrogen-, and phosphoruscontaining borafluorenate hereterocycles (Figure 1B). Compounds containing four- (BN₂P, BNPC, P₂N₂) and fivemembered (BNP₂C and BN₂PC) rings were formed in a facile manner using inexpensive and commercially available pyridylphosphine and bis(phosphine) ligands. Depending on the ligand employed and the orientation of the phosphine donors, heterocycles with varying substitution patterns were obtained. Notably, while mono(phosphine) ligands led to compounds with an exocyclic phosphinimine moiety (Figure 1A), the use of bis(phosphine) or pyridylphosphine results in compounds with endocyclic phosphorus atoms (Figure 1B), leading to a new method to obtain BNP-containing heterocycles. In addition to smaller fused ring compounds, a planar, multiheterocyclic system fused in a 6-5-4-5-6 fashion was obtained when diphenyl-2-pyridylphosphine was used as the coordinating ligand. Theoretical studies were carried out to understand the reaction mechanism as well as the electronic structures of all new compounds.

■ RESULTS AND DISCUSSION

Diphenyl-2-pyridylphosphine (PyPh₂P) is a commonly utilized phosphine ligand that is able to bind transition metal and main group elements in a monodentate (P-bound) or bidentate (Pand N-bound) fashion. 58-60 Due to this coordinative flexibility, we sought to understand how PyPh₂P would react with the Lewis acidic 9-bromo-9-borafluorene (BF-Br). When the two reagents were combined in toluene (1:1 ratio), the corresponding PyPh₂P-borafluorene-bromide adduct 1 was obtained as a white solid in 95% isolated yield (Scheme 1). Although pyridine has been shown to form stable adducts with tricoordinate borafluorenes, 7,56,61,62 the more strongly donating phosphine preferentially binds to borafluorene and the coordination of the pyridine moiety to a second 9-bromo-9borafluorene is disfavored by steric limitations. However, when compound 1 and trimethylsilyl azide (TMS-N₃) reacted in toluene, a new B-N=P heterocycle 2 was generated as a light yellow solid in 95% isolated yield via an intramolecular Staudinger-type reaction (Scheme 1). Compound 2 was also obtained by reacting 9-azido-9-borafluorene (BF-N₃) and

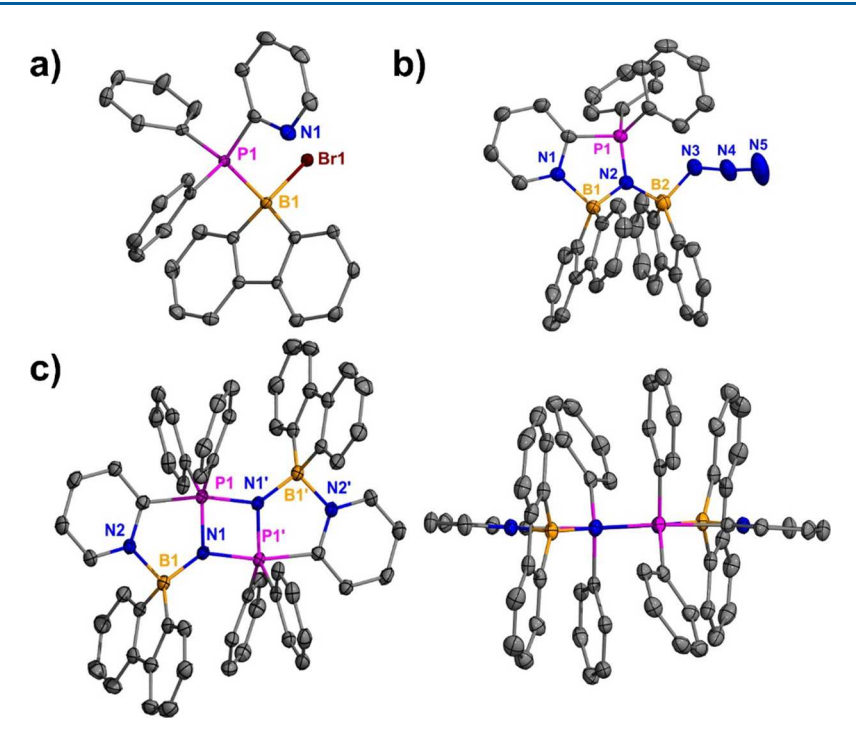


Figure 2. Molecular structures of 1 (a), 2 (b), and 3 (c). Alternate view of 3 in (c) highlights the planarity of the pentaheterocyclic ring system and its orthogonality to the borafluorene moieties. Thermal ellipsoids were set at 50% probability. H atoms and solvent molecules were omitted for the sake of clarity. Selected bond distances [Å] and angles $[^{\circ}]$: 1: B1-P1 2.002(3), B1-Br1 2.051(3), B1-C1 1.597(4); 2: B1-N1 1.637(5), B1-N2 1.560(5), B2-N2 1.599(5), B2-N3 1.605(5), P1-N2 1.587(3), N1-B1-N2 100.7(3), B1-N2-P1 114.7(3), B2-N2-P1 122.5(2), B1-N2-B2 122.8(3), N2-B2-N3 103.2(3); 3: B1-N1 1.529(4), B1-N2 1.607(4), P1-N1 1.654(2), P1-N1' 1.814(2).

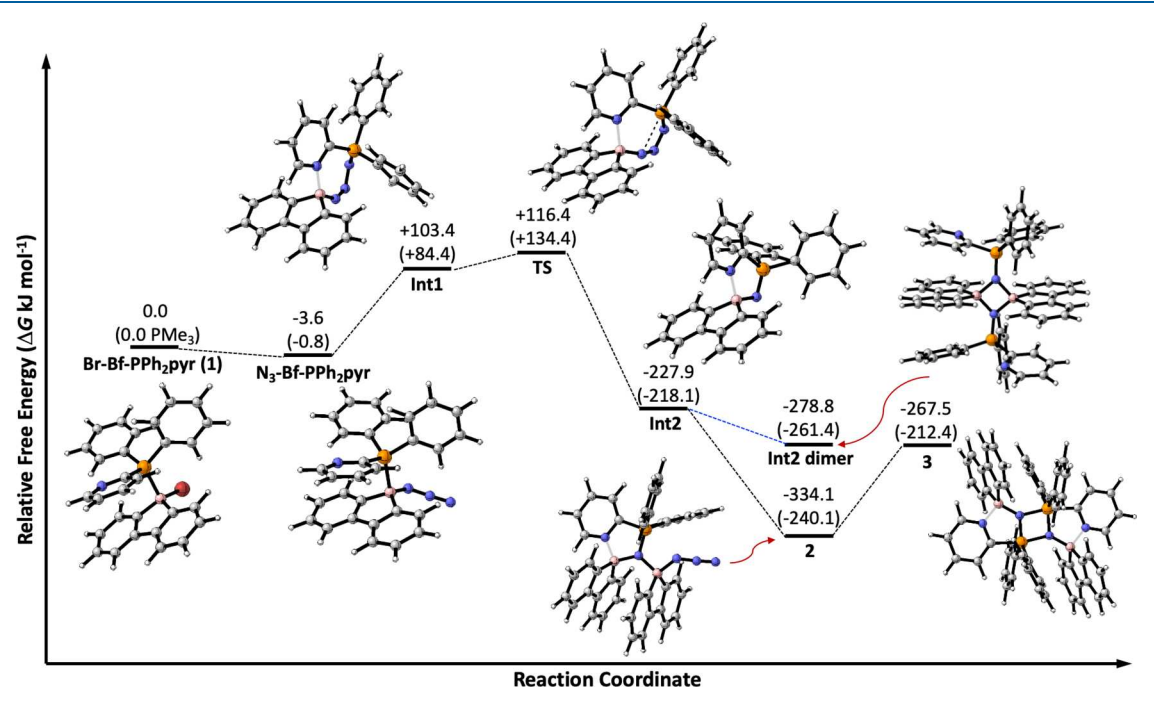


Figure 3. Calculated reaction pathway (ΔG , kJ mol⁻¹) for the thermolysis reaction from 1 to 3. PBE0-D3(BJ)/def2-TZVPP(CPCM,toluene)// PBE0-D3(BJ)/def2-SVP(CPCM,toluene) results were relative to PyPh₂P-BF-Br. Results for Me₃P are provided in parentheses (relative to those for Me₃P-BF-Br).

 $PyPh_2P$ in toluene, albeit in a slightly lower yield (87%). The reactions involved release of dinitrogen (N_2), phosphine transfer from B to N, and formation of a new five-membered BN_2PC ring. Concomitantly, the remaining azide N atom coordinates to a second $BF-N_3$ unit. Compound 2 shows a strong IR spectroscopic absorption band at 2095 cm⁻¹,

corresponding to the $-N_3$ asymmetric stretching vibrations, which are comparable to our reported monodentate phosphine-stabilized borafluorene azides (2095–2105 cm⁻¹)^{48,63} and Bettinger's pyridine- and t-butylpyridine-coordinated borafluorene azides (2125 and 2116 cm⁻¹, respectively).⁷

Analysis of the product by single crystal X-ray diffraction revealed a short P–N bond [1.587(3) Å]. The P–N bond in 2 is consistent with known boron-phosphinimine compounds (1.578–1.607 Å and bond orders of 1.37–1.57), $^{48,50-53}$ which is indicative of P=N double-bond character in 2. PBE0-D3(BJ)/def2-TZVPP(CPCM,toluene)//PBE0-D3(BJ)/def2-SVP(CPCM,toluene) yields a B– Py N distance of 1.610 Å (Mayer bond order of 0.73) with a P–N distance of 1.608 Å (bond order of 1.49). Natural Bond Orbital (NBO) calculated Wiberg bond indices (WBI) underestimate the P–N bond order (1.02–1.05). The presence of a P=N double bond evidenced by the crystal structure and the calculated bond order supports the oxidation of P^{III} to P^V (Figure 2).

When a C_6D_6 solution of complex 2 was refluxed for 4 days, the solution changed from light yellow to brown. The 9-azido-9-borafluorene unit dissociated from the cyclic BNP N atom and a novel BNP-doped bis(borafluorene) heterocycle 3 was obtained in 60% isolated yield (Scheme 1). ¹H and ¹¹B{¹H} NMR spectroscopic analysis of the reaction mixture confirmed the loss of one equivalent of 9-azido-9-borafluorene followed by further oligomerization. Confirmation of oligomerization was completed by refluxing free 9-azido-9-borafluorene for 4 days in C₆D₆ and comparing the corresponding spectroscopic data (¹H and ¹¹B{¹H}) with the reaction mixture obtained during the synthesis of compound 3. It is noteworthy that compound 3 is air-stable. This was confirmed by exposing the solid to air for 2 days and then collecting the solution NMR spectra (1H, 13C, 11B{1H}, and 31P) of the air-exposed compound. No major change was observed compared to the original spectra. Compound 3 was characterized by single crystal X-ray diffraction (Figure 2). The plane of the two borafluorene moieties is orthogonal to the planar BNP pentaheterocyclic core, and the pyridyl rings display displaced π - π stacking with a neighboring molecule of 3 (Figure S38). Moreover, the phosphorus center changes from a tetrahedral geometry in 2 to a distorted trigonal bipyramidal geometry in 3 (Figure 2c). A PBE0-D3(BJ)/def2-TZVPP(CPCM,toluene)// PBE0-D3(BJ)/def2-SVP(CPCM,toluene) optimized geometry of 3 yields a rhomboid P₂N₂ cycle with short (P1-N1 1.667) and long (P1-N1' 1.834 Å) phosphorus-nitrogen bonds, consistent with that in the experimental structure [P1-N1 1.654(2) Å; P1-N1′ 1.814(2) Å]. The Mayer bond orders are 1.26 and 0.81 (cf. 1.49 in 2), which suggest significant P=N character in the shorter P-N bonds, although the bond order is lower than in 2.

A PBE0-D3(BJ)/def2-TZVPP(CPCM,toluene)//PBE0-D3(BJ)/def2-SVP(CPCM,toluene) mechanistic study was carried out for the formation of 2 and 3 (Scheme 1), including a comparison to phosphines (PR₃) with noncoordinating R groups. 48 The calculated reaction energy pathway is illustrated in Figure 3 using both PyPh₂P and Me₃P. The fact that 2 is produced from either BF-N₃ or 1, together with the structure of 2, is suggestive of intramolecular Staudinger reactivity. In our previous study of R₃P reactivity, no products analogous to 2 and 3 were isolated; here, we have investigated the different reactivity observed with a coordinating Py group in PyPh₂P. While not shown in Figure 3, ΔG for the initial addition of PyPh₂P to BF-Br is favorable, calculated to be $-65.0 \text{ kJ mol}^{-1}$ (-101.2 kJ mol⁻¹ with PMe₃). While subsequent replacement of Br by N₃ to form PyPh₂P-BF-N₃ is also favorable, it is only marginally so at -3.6 kJ mol^{-1} (PMe₃ -0.8 kJ mol^{-1}). The overall formation of 2 from 1 is very favorable, with an ΔG of $-334.1 \text{ kJ mol}^{-1}$ ($-398.9 \text{ kJ mol}^{-1}$ if starting from **BF-Br**).

The reaction pathway represents intramolecular Staudinger reactivity, with initial migration of PyPh2P to the terminal $^{azide}N$ (Int1) followed by migration of P to the ^{a}N and ejection of N₂ leading to Int2. With PyPh₂P, the barrier of P migration to ^aN and ejection of N₂ is only 13.0 kJ mol⁻¹, which is significantly reduced compared to Me₃P (50.0 kJ mol⁻¹) due to the stabilizing effect of the PyN-B interaction. Interestingly, the initial structures PyPh₂P-BF-Br and PyPh₂P-BF-N₃ do not exhibit PyN-B coordination that is present in Int1 and all subsequent species. Reaction of Int2 with BF-N₃ readily yields 2. Int2 could potentially dimerize to Int2 dimer as was observed with R₃P,⁴⁸ which yields a stable minima and is favorable for both R₃P and PyPh₂P. However, with PyPh₂P, formation of 2 is calculated to be thermodynamically favored over dimerization by 55.3 kJ mol⁻¹ in contrast to PMe₃, where dimerization is favored by 21.2 kJ mol⁻¹ (43.8 kJ mol⁻¹ with def2-TZVPPD that was used in our previous study^{48,63}). The different reactivity of R₃P and PyPh₂P is a result of reaction thermodynamics, which arises due to the stabilizing PyN-B interaction with PyPh₂P that is absent in R₃P. The impact of PyN-B coordination is evidenced in the similarity of PyPh₂P-BF-Br and PyPh₂P-BF-N₃ reaction energetics for Me₃P and PyPh₂P where there is no ^{Py}N-B coordination, while for subsequent steps, the PyPh₂P pathway yields a lower barrier and more stable Int2 and 2. The reaction from 2 to 3 is calculated to be endergonic (+66.6 kJ mol⁻¹) by using BF-N₃ as the other product. However, BF-N3 was observed to oligomerize in the synthetic study, which together with the endergonic calculated reaction energy, indicates that using molecular BF-N₃ in this final step does not yield the true thermodynamics. It is not feasible to reliably model the thermodynamics of oligomerization of BF-N₃; however, it must be thermodynamically favorable by at least 67 kJ mol⁻¹ to furnish the observed products. Overall, the reaction pathway is indeed consistent with an intramolecular Staudinger-type reaction, where the novel reactivity is driven by the strong PyN-B coordination that is evident in both BF-N=PPh2Py and 2. Different reactivities may be expected with alkyl/aryl R₃P phosphine ligands.

With the goal of isolating different classes of BNP-doped borafluorenate heterocycles, we explored reactions of bisphosphine trans-1,2-bis(diphenylphosphino)ethylene, bis-(diphenylphosphino)methane, and bis(diphenylphosphino)benzene in similar borafluorene-based reaction sequences. Addition of two equivalents of BF-Br in toluene to trans-1,2bis(diphenylphosphino)ethylene yielded the corresponding bis(phosphine-stabilized borafluorene-bromide adduct) 4 as a white solid in 92% isolated yield (Scheme 2). The reaction of 4 with trimethylsilyl azide in toluene at 110 °C generated a new 4-membered BN₂P-spirocyclic complex 5, which may be described by three possible resonance structures 5a, 5b, and **5c** (Scheme 2). As a result, there is a delocalization of electrons over the N-P-N moiety. The reaction proceeds via release of N₂, the presumed release of trans-1,2-dibromoethene, and the cleavage of the P-C bond. Compounds 4 and 5 were characterized by single crystal X-ray diffraction (Figure 4). Structure 4 shows a trans-orientation of both B–Br bonds. In structure 5, the plane of the borafluorene moiety is orthogonal to the 4-membered BN₂P ring, and the spiro-boron atom adopts a tetrahedral geometry.

PBE0-D3(BJ)/def2-TZVPP(CPCM,toluene)//PBE0-D3(BJ)/def2-SVP(CPCM,toluene) results for 5 yields Mayer

Scheme 2. Synthesis of Bis(phosphine-borafluorene-bromide adduct) 4 and 4-Membered BN₂P-Spirocyclic Complex 5 (Resonance Hybrid) and Resonance Structures 5a-5c

bond orders of 0.75 (B-N), 1.01 (Si-N), and 1.27 (P-N bonds) (cf. 1.49 in 2), which is consistent with less P-N double-bond character compared to 2, yet substantial P-N double-bond character remains that is very similar to the case of the shorter P-N bonds in 3 (bond order 1.26). NBO indicates an absence of any covalent Si-N bonding NBOs; however, lone pair (LP*) NBOs on Si have significant population (0.37 e), and the donor-acceptor interaction (from second order perturbation) from the N lone pair NBO to Si lone pair is 219 kcal/mol, which is suggestive of an ionic N-Si bonding interaction. Natural resonance theory (NRT) analysis yields all single bonds equivalent to 5c (Scheme 2), although the ionic bonding preference with NBO suggests that the NRT results may not provide a reliable description of the bonding. The optimized P-N bond distances (1.627-1.628 Å) are in agreement with Pyykko and Atsumi's empirical covalent double-bond radii for P=N (1.62 Å). 64,65 Similarly, the B-N bond distances (1.611-1.612 Å) are longer than the empirical single bond radii (1.56 Å), while the optimized Si-N bond distances (1.755-1.756 Å) lie between Pyykko and Atsumi's empirical values for double (1.67 Å) and single (1.87 Å) bonds. The longer B–N bonds (with smaller bond order) are suggestive of a weaker B-N interaction because of the substantial P=N character. Hirshfeld atomic charges of P (+0.41), B (+0.06), N (-0.27), and Si (+0.34) with a negative charge on N indicate some electron density accumulation, consistent with partial lone pair presence. It is suggested that all resonance structures 5a-5c contribute to the description of bonding, with the P-N Mayer bond order of 1.27 (cf. 1.29 in 3) indicating that 5a-5b (with P=N) are the dominant resonance structures. Calculated ΔG for the formation of 4 and 5 according to Scheme 2 is calculated to be very favorable: -154.2 kJ mol⁻¹ for the formation of 4 and -899.5 kJ mol⁻¹ for the subsequent step to form 5.

Addition of bis(diphenylphosphino)methane to two equivalents of 9-bromo-9-borafluorene in toluene yielded bis-(phosphine-stabilized borafluorene-bromide adduct) **6** as a white solid in 90% yield (Scheme 3). Compound **6** was successfully characterized by single crystal X-ray diffraction, and both B–Br bonds are oriented in a cis fashion (Figure 5). It is noteworthy that this dramatically alters the solubility, with adduct **4** having relatively poor solubility in organic solvents

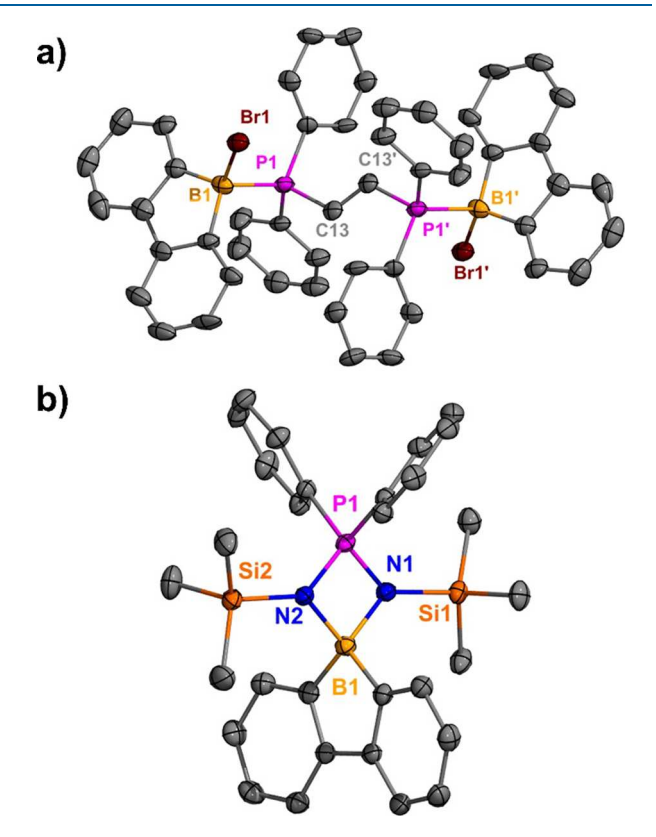


Figure 4. Molecular structures of 4 (a) and 5 (b). Thermal ellipsoids set at 50% probability and H atoms were omitted for clarity. Selected bond distances [Å]: 4: B1–Br1 2.054 (2), B1–P1 1.976(3). 5: B1–N1 1.629(3), B1–N2 1.629(3), P1–N1 1.6112(17), P1–N2 1.6086(18).

such as hexanes, toluene, DCM, and THF compared to that of 6. When 6 reacts with trimethylsilyl azide at room temperature in toluene for 15 h, a new BNPC-heterocycle 7 is formed (Scheme 3). Compound 7 shows a strong IR absorption band at 2095 cm⁻¹ corresponding to the -N₃ asymmetric stretching vibrations, which is comparable to that in compound 2 and reported boron azides.^{7,48,63} Additionally, it was fully characterized by NMR spectroscopy (¹H, ¹³C, ¹¹B{¹H}, and

Scheme 3. Synthesis of Bis(phosphine-borafluorene-bromide) Adduct 6, BN_2PC -Heterocycle 7, and Chiral BNPC-Spirocyclic Complex 8

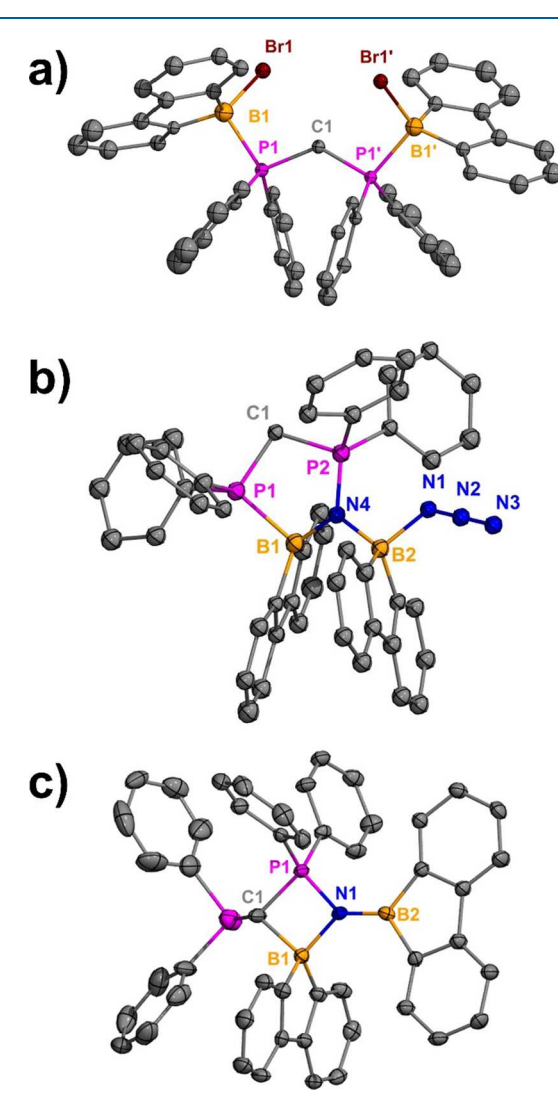


Figure 5. Molecular structures of **6** (a), 7 (b), and **8** (c). Thermal ellipsoids set at 50% probability. H atoms and solvent were omitted for clarity, as was the minor position of the disordered atoms in **8**. While the atom connectivity in 7 is established by X-ray diffraction, the geometrical parameters are not discussed due to insufficient crystal quality. Selected bond distances [Å]: **6**: B1–Br1 2.065 (4), B1–P1 1.970(5); **8**: B1–N1 1.415(4), B1–C1 1.573(4), C25–P1 1.792(1), P1–N1 1.640(2), B2–N1 1.627(4).

³¹P) and confirmed by elemental analysis (EA). The ¹¹B{¹H} NMR spectrum gives two resonances at 15.0 and -4.1 ppm, corresponding to two tetracoordinate boron centers. While the structure of compound 7 indicates connectivity (Figure 5), poor crystal quality prevents a detailed discussion of the geometrical data. When complex 7 was heated at reflux in toluene for 2 days, the chiral 4-membered BNPC-spirocyclic compound 8 formed via ring contraction. The reaction may

have proceeded by the initial release of azide anion (-N₃) which then deprotonated one of the protons of the phosphine ligand to produce hydrazoic acid (HN₃). It is noteworthy that this reaction needs to be run with careful attention due to the presumed release of the explosive and highly toxic HN₃ (see Experimental Section for additional information). Complex 8 was successfully characterized by single crystal X-ray diffraction (Figure 5). The tricoordinate borafluorene moiety is in the same plane as the 4-membered BNPC ring, while the tetracoordinate borafluorene is orthogonal to the BNPC ring. We note that compound 8 is air-stable in the solid state. Its stability was verified by allowing it to be in contact with air for a period of 3 days. Subsequently, solution NMR data (1H, 13C, $^{11}\overline{B}\{H\}$, and $^{31}P)$ were collected from the exposed compounds, revealing no significant change compared to their original spectra.

The calculated energetics for the first step of Scheme 3 to form 6 give a ΔG of -174.7 kJ mol $^{-1}$. Subsequent replacement of Br by N₃ from 6 is only favorable by 11.2 kJ mol $^{-1}$, although subsequent loss of N₂ to form 7 is very thermodynamically favorable (-264.3 kJ mol $^{-1}$). The calculated ΔG for the final step to produce 8 is +95.9 kJ mol $^{-1}$. While a TS could not be located to confirm the reaction pathway, the energetics are consistent with the required reaction conditions reported in Scheme 3. It is noted that 7 has a similar structure to 2 (Scheme 1), with coordination of P to the B of borafluorene; however, the formation of an analog of 3 with diphosphine is not favored.

Unexpectedly, the addition of bis(diphenylphosphino)benzene to two equiv of 9-bromo-9-borafluorene in toluene did not yield a Lewis acid-base adduct as was the case with the other bis(phosphines) used in this study (Schemes 2 and 3). Instead, [bis(diphenylphosphino)benzene]-stabilized borafluoronium ion 9 was formed, with an unusual borafluorene dibromide ion pair (Scheme 4 and Figure 6). We attribute the formation of the cationic borafluorene species to the cisorientation of the two phosphine ligands on the benzene linker, which forces them to bind to the same electrophilic boron center. When compound 9 reacts with two equivalents of TMS-N₃, the borafluoronium ion stays intact, while the anion undergoes a double displacement reaction to form a borafluorene diazide anion 10 (Scheme 4). The ¹¹B{¹H} NMR spectrum of 9 gives two resonance peaks at -1.8 ppm (anion) and -15.4 ppm (cation) in CD_2Cl_2 . Due to the limited solubility of 10 compared to that of 9, the ¹¹B{¹H} NMR spectrum of 10 was taken in THF-D₈ which shows two resonances at 0.6 and -13.9 ppm. The ¹¹B{¹H} NMR spectra of the borafluoronium ions in 9 (-15.4 ppm) and 10 (-13.9 m)ppm) are significantly different compared to our reported monodentate carbene- and carbone-stabilized borafluorenium ions, 39,40 where peaks are typically downfield in the range of 48-66 ppm. Both compounds 9 and 10 are air-stable in solution and solid states. There were no changes as determined

Scheme 4. Synthesis of Diphosphine-Stabilized Borafluoronium Ions 9-10.

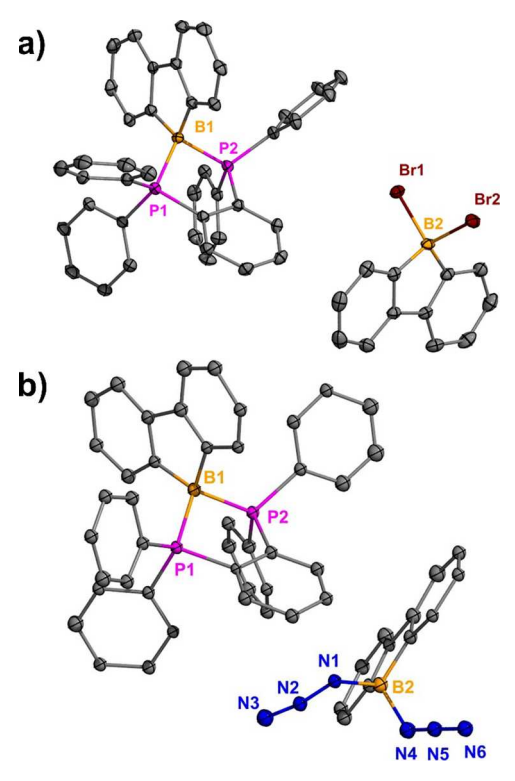


Figure 6. Molecular structures of **9** (a) and **10** (b). Thermal ellipsoids set at 50% probability. H atoms and solvent molecules were omitted for clarity. Selected bond distances [Å]: **9**: B1-P1 1.979(3), B1-P2 1.972(3), B2-Br1 2.091(3), B2-Br2 2.056(3). **10**: B1-P1 1.966 (3), B1-P2 1.968(3), B2-N1 1.585(4), B2-N4 1.569(4).

by NMR spectroscopy after solutions of **9** and **10** were exposed to air for 3 days. When **10** undergoes thermolysis (120 $^{\circ}$ C) in a pressure tube for 2 days, a complex mixture of products formed, which could not be separated to allow characterization.

The optimized geometry of the free diphosphine-stabilized borafluoronium ion common to 9 and 10 yields B–P bonds with Mayer bond orders of 0.79 (1.966 Å) and 0.82 (1.969 Å), respectively, which is comparable to 0.86 (1.991 Å) in 1. The Mulliken charge on the B center is -0.038 e, which is similar to -0.085 e in 1 and +0.035 e in 2, and much more positive than -0.36 e in 5 and -0.33 e in 3. The unusual BF anions in 9 and 10 exhibit different electronic environments, highlighted by Mulliken charges for B of 0.23 (Br, 9) and -0.08 (N $_3$, 10). PBE0-D3(BJ)/def2-TZVPP(CPCM,toluene)//PBE0-D3(BJ)/def2-SVP(CPCM,toluene) results for the reactivity in Scheme 4 indicate that the formation of [bis(diphenylphosphino)-benzene]-stabilized borafluoronium 9 is thermodynamically favorable by 41 kJ/mol, while further reaction with TMS-N $_3$ to form 10 is favorable by 19 kJ/mol.

We also investigated the molecular orbital plots of the boron heterocyclic compounds 3, 5, and 8, and the common diphosphine-stabilized borafluoronium ion shared by 9 and 10 (Figure 7). In 3, the HOMO is centered on the

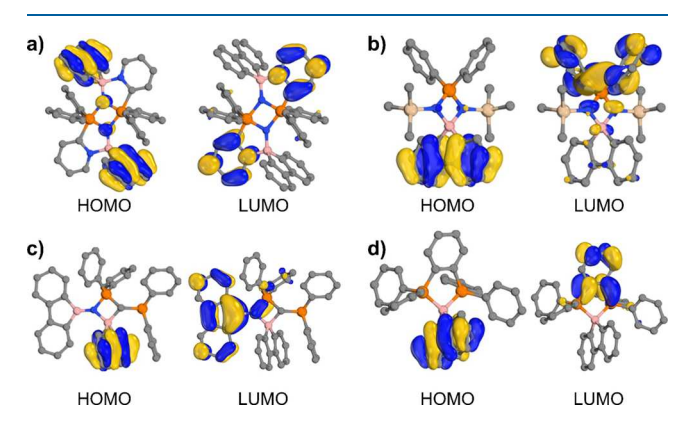


Figure 7. Plots of the HOMO and LUMO of 3 (a), 5 (b), 8 (c), and 9/10 (d). PBE0-D3(BJ)/def2-TZVPP(CPCM,toluene)//PBE0-D3(BJ)/def2-SVP(CPCM,toluene).

borafluorene moieties, while the LUMO is centered on the pyridyl substituents. As for 5, the HOMO is also located on the borafluorene unit, and the LUMO is on the two phenyl substituents attached to the phosphorus center. The HOMO in 8 is centered on the tetracoordinate borafluorene moiety, while the LUMO is centered on the tricoordinate borafluorene moiety, which primarily involves the vacant p orbital of boron. For the diphosphine-stabilized borafluorenium ion in 9 and 10, the HOMO is centered on the borafluorene moiety with π character, while the π^* LUMO is distributed over both the benzene ring and the phosphorus centers (Figure 7d). Overall, it is noted that the HOMO centered on the borafluorene moiety is common for all borafluorene compounds 3, 5, 8, and 9–10.

CONCLUSIONS

We highlight a versatile pyridylphosphine and bis(phosphine) ligand strategy that has been used to synthesize an array of new boron, nitrogen, and phosphorus-containing heterocycles via intramolecular Staudinger-type reactions. The newly synthesized compounds have diverse heteroatom substitution patterns and ring fusions and/or connectivities. While diphenyl-2-pyridylphosphine (PyPh₂P), trans-1,2-bis-(diphenylphosphino)ethylene (Ph₂PHC=CHPPh₂), and bis-(diphenylphosphino)methane (Ph₂PCH₂PPh₂) all led to compounds where the phosphines bind in a bis(monodentate) fashion, bis(diphenylphosphino)benzene exceptionally generated the bidentate diphosphine-stabilized borafluoronium ion with unusual tetracoordinate borafluorene dibromide and diazide anions. Theoretical calculations were conducted to understand potential mechanisms for the formation and

electronics of the boracycles, which clearly showed unique reaction pathways and configurations based on the specific ligand employed. The use of the bis(monodentate) and bidentate ligand approach to access new borafluorene compounds may have broad implications in the design of borafluorenes with extended π -systems and supramolecular structures, which is an aspect of borafluorene chemistry that remains underdeveloped. ¹

EXPERIMENTAL SECTION

General Procedures. All air- and moisture-sensitive reactions were performed under an inert atmosphere of argon using standard Schlenk techniques or in a MBRAUN LABmaster glovebox equipped with a -37 °C freezer. Reaction solvents including toluene and hexanes were purified by distillation over sodium, while ethereal solvents such as diethyl ether and tetrahydrofuran (THF) were purified by distillation over Na/benzophenone. Deuterated solvents were purchased from Acros Organics and Cambridge Isotope Laboratories and dried over sodium (C₆D₆) or Na/K alloy (THFd₈). All glassware used for reactions was oven-dried at 190 °C overnight. The NMR spectra were recorded at 298.15 K on a Varian 600 MHz spectrometer. Proton and carbon chemical shifts are reported in ppm and are referenced using the residual proton and carbon signals of the deuterated solvent (${}^{1}\text{H}$: C₆D₆ δ = 7.16, THF- d_8 $\delta = 3.58, 1.72;$ ¹³C: C₆D₆ $\delta = 128.06, \text{THF-}d_8 \delta = 67.21, 25.31$). All boron signals are reported in ppm and were referenced to an external standard, BF₃·Et₂O (11 B: $\delta = 0.00$). Due to a borosilicate NMR probe, there is a broad signal observed from -25 to 25 ppm. ³¹P NMR chemical shifts were referenced to an 85% phosphoric acid standard (31P: δ = 0.00). Single crystal X-ray diffraction data collection and structure refinement details are given in the X-ray crystallographic section of the Supporting Information. Elemental analyses were performed at the University of Virginia Department of Chemistry by using a PerkinElmer 2400 Series II analyzer. The following compounds were prepared according to literature procedures: 9halo-9-borafluorene.^{7,40} and 9-azido-9-borafluorene.^{7,8,66} All other compounds were purchased from Sigma-Aldrich and Fisher Scientific and used without further purification.

CAUTION: The azides used and described in this report may be shock-sensitive and/or explosive. With the exception of the air-stability tests, they were handled under an inert atmosphere (i.e., a glovebox or Schlenk line). Before attempting to synthesize or handle these compounds, researchers should familiarize themselves with the materials safety data sheets (MSDS) for azide compounds and adhere to appropriate safety guidelines.

Synthesis of Compound 1. To a mixture of 9-bromo-9borafluorene (0.41 mmol, 128.00 mg) and diphenyl-2-pyridylphosphine (0.49 mmol, 129.00 mg), 20 mL of toluene was added. The resulting mixture was allowed to stir for 4 h. All volatile components were removed in vacuo, and the remaining solid was washed with 10 mL of hexanes and dried to afford the product was isolated as a white solid (197.16 mg, 95% yield). ¹H NMR (600 MHz, C₆D₆) δ 8.20 (d, J = 2.2 Hz, 2H), 7.83 (d, J = 7.2 Hz, 2H), 7.71 (t, J = 9.2 Hz, 4H), 7.45 (d, J = 7.5 Hz, 2H), 7.14 (d, J = 7.5 Hz, 2H), 7.10 (t, J = 6.7 Hz, 2H),6.92 (t, J = 7.4 Hz, 2H), 6.88-6.79 (m, 5H), 6.43-6.37 (d, 1H) ppm. 13 C NMR (151 MHz, C_6D_6) δ 152.58 (ArC), 152.06 (ArC), 150.47 (ArC), 150.37 (ArC), 149.53 (ArC), 149.48 (ArC), 135.61 (ArC), 135.55 (ArC), 135.09 (ArC), 135.05 (ArC), 133.12 (ArC), 131.66 (ArC), 131.64 (ArC), 126.85 (ArC), 125.76 (ArC), 125.36 (ArC), 125.05 (ArC), 119.84 (ArC) ppm. $^{11}B\{^{1}H\}$ NMR (192 MHz, C_6D_6) δ -7.4 ppm. $^{31}P\{^{1}H\}$ NMR (243 MHz, $^{C}_{6}D_{6}$) δ 1.42 ppm. Anal. Calcd For C₂₉H₂₂BBrNP: C, 68.81; H, 4.38; N, 2.77%. Found C, 68.90; H, 4.38; N, 2.73%.

Synthesis of Compound 2. Route 1: To a solution of $PyPh_2P-BF-Br$ adduct 1 (0.220 mmol, 0.110 g) in toluene, pure trimethylsilyl azide (7.60 mmol, 2.00 mL) was added. After the addition of TMS-N₃, the clear solution turned pale yellow. The reaction mixture was stirred for 3 h. All volatile components were removed in vacuo, and

the remaining solid was washed with hexanes and toluene and then dried to give the product as a light yellow solid (0.134 g, 95% yield).

Route 2: To a solution of 9-azido-9-borafluorene (0.83 mmol, 0.0780 g) in toluene, diphenyl-2-pyridylphosphine (1.24 mmol, 0.326 g) was added. The reaction mixture was stirred for 2 h. All volatile components were removed in vacuo, and the remaining solid was washed with hexanes and toluene and then dried to afford the product as a light yellow solid (466 mg, 87% yield). ¹H NMR (600 MHz, C_6D_6) δ 8.49 (d, J = 4.8 Hz, 1H), 7.50 (t, J = 6.9 Hz, 3H), 7.15–7.14 (m, 2H), 7.13 (q, J = 1.2 Hz, 5H), 7.12-7.12 (m, 3H), 7.06 (d, J =1.0 Hz, 4H), 7.05 (d, J = 0.7 Hz, 2H), 7.02-7.02 (m, 4H), 7.01-7.00(m, 4H), 6.86 (t, J = 7.7 Hz, 1H), 6.50 (dd, J = 7.6, 4.7 Hz, 1H) ppm. 13 C NMR (151 MHz, C_6D_6) δ 164.48 (ArC), 150.47 (ArC), 150.40 (ArC), 137.36 (ArC), 135.32 (ArC), 134.79 (ArC), 134.66 (ArC), 129.34 (ArC), 129.10 (ArC), 128.81 (ArC), 128.76 (ArC), 128.56 (ArC), 125.70 (ArC), 122.07(ArC) ppm. 11B{1H} NMR (192 MHz, THF- d_8) δ 10.1, 3.3 ppm. ³¹P{¹H} NMR (243 MHz, C₆D₆) δ : -3.54 ppm. Anal. Calcd For C₄₁H₃₀B₂N₅P: C, 76.31; H, 4.69; N, 10.85%. Found C, 76.62; H, 4.52; N, 10.73%.

Synthesis of Compound 3. A solution of compound 2 (0.0780 mmol, 50 mg) in C₆D₆ solvent was refluxed for 4 days in a J-Young tube. The solution changed from light yellow to brown. The reaction was tracked by using 11B{1H} and 31P{1H} NMR to confirm conversion to the desired product after 4 days. The C₆D₆ solvent was removed in vacuo, and the remaining solid was redissolved in THF and then concentrated for recrystallization at room temperature to obtain colorless crystals (20 mg, 60% yield). ¹H NMR (600 MHz, THF- d_8) δ 8.69–8.58 (m, 3H), 8.27 (t, J = 9.3 Hz, 1H), 8.02–7.67 (m, 7H), 7.54 (s, 3H), 7.44-7.36 (m, 14H), 7.31 (d, J = 4.7 Hz,10H), 7.16 (d, J = 12.8 Hz, 3H), 7.09 (d, J = 7.8 Hz, 3H). ¹³C NMR (151 MHz, THF-D₈) δ 151.10 (ArC), 138.23 (ArC), 136.34 (ArC), 135.23 (ArC), 133.16 (ArC), 131.61 (ArC), 129.69 (ArC), 129.32 (ArC), 129.27 (ArC), 128.89 (ArC), 128.73 (ArC), 122.98 (ArC). ¹¹B{¹H} NMR (192 MHz, C_6D_6) δ -6.5 ppm. ³¹P{¹H} NMR (243 MHz, THF- d_8) δ : 15.00 ppm. $C_{58}H_{44}B_2N_4P_2$: C, 79.11; H, 5.04; N, 6.36%. Found C, 79.55; H, 5.40; N, 5.98%.

Synthesis of Compound 4. To a solution of 9-bromo-9borafluorene (1.24 mmol, 0.300 g) in toluene, trans-1,2-bis-(diphenylphosphino)ethylene (0.618 mmol, 0.255 g) was added. The resulting mixture was allowed to stir for 8 h. All volatile components were removed in vacuo, and the remaining solid was washed with 10 mL of toluene and dried to give the product as a white solid (0.528 g, 92% yield). ¹H NMR (600 MHz, CD_2Cl_2) δ 7.65-7.52 (m, 2H, ArH), 7.45-7.41 (m, 6H, ArH), 7.36 (d, J = 8.5Hz, 4H), 7.26-7.23 (m, 8H, ArH), 7.17 (d, J = 6.7 Hz, 12H, ArH), 7.14 (s, 4H, ArH), 6.97 (d, J = 8.1 Hz, 2H, HC = CH). ¹³C NMR (151 MHz, TCE- d_2) δ 148.34 (ArC), 138.02 (ArC), 133.78 (ArC), 132.60 (ArC), 131.89 (ArC), 129.19 (ArC), 128.36 (ArC), 125.46 (ArC), 119.82 (ArC), 21.62 (PHC=CHP) ppm. ¹¹B{¹H} NMR (192 MHz, TCE- d_2) δ –16.1 ppm. ³¹P{¹H} NMR (243 MHz, TCE- d_2) δ -0.66 ppm. Anal. Calcd For C₅₀H₃₈B₂Br₂P₂:C, 68.07; H, 4.34%. Found C, 68.32; H, 4.71%.

Synthesis of Compound 5. To a solution of compound 4 (0.164 mmol, 0.150 mg) in toluene was added an excess amount of trimethylsilyl azide (1.64 mmol, 0.189 g, 0.220 mL). The reaction mixture was heated at 110 °C for 1 day. All volatile components were removed in vacuo, and the remaining solid was washed with hexanes and then dried to afford the product as a light yellow solid (0.0642 g, 75% yield). ¹H NMR (600 MHz, THF- d_8) δ 8.12–7.94 (m, 3H, ArH), 7.75 (m, 3H, ArH), 7.51–7.40 (m, 6H, ArH), 7.25 (m, 3H, ArH), 7.11–7.01 (m, 3H, ArH), 0.22 – -0.22 (m, 18H, Si–CH). ¹³C NMR (151 MHz, THF- d_8) δ 133.38 (ArC), 132.30 (ArC), 129.34 (ArC), 128.72 (ArC), 126.52 (ArC), 118.96 (ArC), 1.13 (Si–C). ¹¹B{¹H} NMR (192 MHz, THF- d_8) δ 1.0 ppm. ³¹P{¹H} NMR (243 MHz, THF- d_8) δ 52.87 ppm. Anal. Calcd For C₃₀H₃₆BN₂PSi₂: C, 68.95; H, 6.94; N, 5.36%. Found C, 68.78; H, 7.10; N, 5.92%.

Synthesis of Compound 6. To a solution of 9-bromo-9-borafluorene (1.24 mmol, 0.300 g) in toluene, bis-(diphenylphosphino)methane (0.618 mmol, 0.237 g) was added. The resulting mixture was allowed to stir for 8 h. All volatile

components were removed in vacuo, and the remaining solid was washed with 10 mL of toluene and then dried to afford the product as a white solid (0.492 g, 90% yield). $^1\mathrm{H}$ NMR (600 MHz, C_6D_6) δ 7.86 (d, J=7.0 Hz, 4H, BF-ArH), 7.35 (d, J=6.9 Hz, 4H, BF-ArH), 7.20 (m, 6H, ArH), 7.15–7.12 (m, 8H, ArH), 7.08–6.99 (m, 4H, BF-ArH), 6.69 (m, 4H, BF-ArH), 6.52 (m, 6H, ArH), 4.73 (s, 2H, P–CH–P). $^{13}\mathrm{C}$ NMR (151 MHz, C_6D_6) δ 153.14 (ArC), 133.41 (ArC), 132.91 (ArC), 132.47 (ArC), 128.88 (ArC), 128.63 (ArC), 128.35 (ArC), 120.10 (ArC), 18.89 (P–CH–P) ppm. $^{11}\mathrm{B}\{^1\mathrm{H}\}$ NMR (192 MHz, C_6D_6) δ –6.0 ppm. $^{31}\mathrm{P}\{^1\mathrm{H}\}$ NMR (243 MHz, THF- d_8) δ 2.51 ppm. Anal. Calcd For $C_{49}\mathrm{H}_{38}\mathrm{B}_2\mathrm{Br}_2\mathrm{P}_2$:C, 67.63; H, 4.40%. Found C, 67.35; H, 4.23%.

Synthesis of Compound 7. To a solution of 6 (0.226 mmol, 0.200 g) in toluene was added an excess of trimethylsilyl azide (2.26 mmol, 0.260 g 0.300 mL). The reaction mixture was stirred for 15 h. All volatile components were removed in vacuo, and the remaining solid was washed with hexanes and then dried to give the product was isolated as a light yellow solid (0.155 g, 90% yield). ¹H NMR (600 MHz, C_6D_6) δ 7.62 (d, J = 7.2 Hz, 4H), 7.31 (d, J = 7.5 Hz, 4H), 7.19 (d, J = 7.9 Hz, 8H), 7.11 (d, J = 7.5 Hz, 4H), 7.01 (t, J = 7.7 Hz, 4H),6.88 (t, J = 7.3 Hz, 4H), 6.79 (t, J = 7.6 Hz, 8H), 3.22 (s, 2H). ¹³C NMR (151 MHz, C_6D_6) δ 150.88 (ArC), 133.39 (ArC), 133.29 (ArC), 131.90 (ArC), 131.85 (ArC), 130.44 (ArC), 130.37 (ArC), 128.57 (ArC), 128.52 (ArC), 127.32 (ArC), 120.07 (ArC), 19.75 (P-CH-P) ppm. $^{11}B\{^{1}H\}$ NMR (192 MHz, $C_{6}D_{6}$) δ 15.0, -4.1 ppm. $^{31} P\{^{1} H\}$ NMR (243 MHz, THF-D_8) δ 0.23, —28.33 ppm. Anal. Calcd For C₄₉H₃₈B₂N₄P₂: C, 76.79; H, 5.00; N, 7.31%. Found C, 76.75; H, 4.83; N, 7.47%.

Synthesis of Compound 8. A solution of 7 (0.131 mmol, 0.100 g) in toluene was refluxed for 2 days in a pressure tube. The reaction was tracked using ¹¹B{¹H} and ³¹P{¹H}NMR spectroscopies to confirm conversion to the desired product after 2 days. All volatile components were removed in vacuo, and the remaining solid was washed with hexanes and then dried to afford the product as a white solid (0.663 g, 70% yield). Note: Due to presumed formation of HN₃, this reaction was conducted in a closed system or pressure tube outside of the glovebox. Then, the pressure tube was brought in the glovebox (inert atmosphere) after 2 days where the purification and work up were conducted safely. ¹H NMR (600 MHz, C₆D₆) δ 8.21 (m, 1H, ArH), 7.98-7.90 (m, 2H, ArH), 7.79 (m, 1H, ArH), 7.69-7.63 (m, 4H, ArH), 7.50-7.42 (m, 2H, ArH), 7.38-7.32 (m, 2H, ArH), 7.24-7.20 (m, 2H, ArH), 7.13 (d, J = 1.4 Hz, 2H, ArH), 7.10-7.07 (m, 2H, ArH), 7.06 (d, J = 1.6 Hz, 2H, ArH), 7.01 (d, J = 6.9 Hz, 4H, ArH), 6.97-6.95 (m, 2H, ArH), 6.91 (s, 2H, ArH), 6.82 (s, 4H, ArH), 6.77–6.73 (m, 2H, ArH), 6.70–6.67 (m, 2H, ArH), 3.26 (d, J = 13.5 Hz, 1H, PCH). ${}^{11}B\{{}^{1}H\}$ NMR (192 MHz, C_6D_6) δ 12.6, -10.8 ppm. ${}^{31}P\{{}^{1}H\}$ NMR (243 MHz, C_6D_6) δ 28.32, -22.23 ppm. C₄₉H₃₇B₂NP₂: C, 81.36; H, 5.16; N, 1.94%. Found C, 81.74; H, 5.25; N, 2.05%.

Synthesis of Compound 9. To a solution of 9-bromo-9borafluorene (0.823 mmol, 0.200 g) in toluene was added bis(diphenylphosphino)benzene (0.412 mmol, 0.184 g). The resulting mixture was allowed to stir for 8 h. All volatile components were removed in vacuo, and the remaining solid was washed with 10 mL of a hexanes/toluene (1:1) mixture and then dried to give the product a white solid (357 mg, 93% yield). ¹H NMR (600 MHz, CD_2Cl_2) δ 8.20 (m, 2H), 8.14 (m, 2H, ArH), 7.88 (d, J = 7.6 Hz, 2H, ArH), 7.63-7.56 (m, 1H, ArH), 7.49 (m, 7H, ArH), 7.29 (t, J = 8.1Hz, 8H, ArH), 7.24 (t, J = 7.8 Hz, 2H, ArH), 7.20-7.12 (m, 2H, ArH), 7.09 (q, J = 5.7 Hz, 12H, ArH), 6.83 (d, J = 7.3 Hz, 2H, ArH) ppm. 13 C NMR (151 MHz, CD₂Cl₂) δ 150.97 (ArC), 136.07 (ArC), 135.72 (ArC), 133.76 (ArC), 133.08 (ArC), 130.93 (ArC), 129.72 (ArC), 129.35 (ArC), 128.54 (ArC), 127.21 (ArC), 126.96 (ArC), 126.78 (ArC), 125.62 (ArC), 122.32 (ArC), 121.85 (ArC), 121.50 (ArC) ppm. 11 B NMR (192 MHz, CD₂Cl₂) δ –1.8, –15.4 ppm. 31 P NMR (243 MHz, CD_2Cl_2) δ 10.29 ppm. Anal. Calcd For C₅₄H₄₀B₂Br₂P₂:C, 69.57; H, 4.32%. Found C, 69.96; H, 4.50%.

Synthesis of Compound 10. To a solution of compound 9 (0.333 mmol, 0.300 g) in toluene was added excess trimethylsilyl azide (3.33 mmol, 0.40 mL). The reaction mixture was stirred for 4 h. All volatile

components were removed in vacuo, and the remaining solid was washed with hexanes and then dried to afford the product as a white solid (274 mg, 95% yield). $^1{\rm H}$ NMR (400 MHz, C_6D_6) δ 8.00 (m, 2H, ArH), 7.72 (d, J=7.7 Hz, 2H, ArH), 7.65 (m, 2H), 7.54 (m, 2H, ArH), 7.36 (m, 6H, ArH), 7.23 (m, 6H, ArH), 7.00 (m, 4H, ArH), 6.96 (m, 2H, ArH), 6.92 (m, 4H, ArH), 6.78 (m, 10H, ArH). $^{13}{\rm C}$ NMR (101 MHz, THF-D_8) δ 134.83 (ArC), 134.21 (ArC), 130.83 (ArC), 130.48 (ArC), 130.42 (ArC), 130.36 (ArC), 130.07 (ArC), 129.25 (ArC), 127.63 (ArC), 126.68 (ArC), 126.32 (ArC), 123.70 (ArC), 123.34 (ArC), 121.93 (ArC), 118.95(ArC). $^{11}{\rm B}\{^1{\rm H}\}$ NMR (128 MHz, THF-D_8) δ : -13.9, 0.6 ppm. $^{31}{\rm P}$ NMR (162 MHz, CD_2Cl_2) δ 9.32 ppm. Anal. Calcd For $C_{\rm 54}H_{40}B_{2}N_{6}P_{2}$: C, 75.72; H, 4.71; N, 9.81%. Found C, 75.90; H, 4.69; N, 10.01%.

Theoretical Calculations. All calculations were performed using Orca 5.0.3, ⁶⁷ using the PBE0 density functional, ^{68,69} Grimme's D3 dispersion correction with Becke-Johnson damping, ^{70,71} and the def2-SVP basis set ⁷² — labeled PBE0-D3(BJ)/def2-SVP. All calculations employed the conductor-like polarizable continuum model (CPCM) for solvation with parameters for toluene. ⁷³ The RIJCOSX approximation with a def2/J fitting set was employed for all calculations. ⁷⁴ Minima were confirmed with vibration frequency calculations performed analytically at the same level of theory. Single-point energies, MOs, bond orders, and NBOs were calculated at the PBE0-D3(BJ)/def2-TZVPP⁷² level of theory at the PBE0-D3(BJ)/def2-SVP geometries (all inclusive of solvation). All reported ΔG values are PBE0-D3(BJ)/def2-TZVPP electronic energies, together with PBE0-D3(BJ)/def2-SVP free energy corrections. Transition state optimizations employed the NEB-TS approach. ⁷⁵ All transition states were confirmed to connect relevant minima with intrinsic reaction coordinate (IRC) calculations.

ASSOCIATED CONTENT

Supporting Information

The Supporting Information is available free of charge at https://pubs.acs.org/doi/10.1021/acs.inorgchem.4c00854.

NMR spectra (¹H, ¹³C, ¹¹B{¹H}, and ³¹P) for all compounds, IR spectra, crystallographic and X-ray refinement details, and computational details (PDF)

Accession Codes

CCDC 2242940–2242946 and 2333213–2333214 contain the supplementary crystallographic data for this paper. These data can be obtained free of charge via www.ccdc.cam.ac.uk/data_request/cif, or by emailing data_request@ccdc.cam.ac.uk, or by contacting The Cambridge Crystallographic Data Centre, 12 Union Road, Cambridge CB2 1EZ, UK; fax: +44 1223 336033.

AUTHOR INFORMATION

Corresponding Authors

David J. D. Wilson — Department of Chemistry, La Trobe Institute for Molecular Science, La Trobe University, Melbourne 3086 Victoria, Australia; orcid.org/0000-0002-0007-4486; Email: david.wilson@latrobe.edu.au

Robert J. Gilliard, Jr — Department of Chemistry, Massachusetts Institute of Technology, Cambridge, Massachusetts 02139-4307, United States; oocid.org/ 0000-0002-8830-1064; Email: gilliard@mit.edu

Authors

Bi Youan E. Tra – Department of Chemistry, Massachusetts Institute of Technology, Cambridge, Massachusetts 02139-4307, United States

Andrew Molino – Department of Chemistry, La Trobe Institute for Molecular Science, La Trobe University,

- Melbourne 3086 Victoria, Australia; o orcid.org/0000-0002-0954-9054
- Kimberly K. Hollister Department of Chemistry, Massachusetts Institute of Technology, Cambridge, Massachusetts 02139-4307, United States; orcid.org/ 0000-0001-9024-4436
- Samir Kumar Sarkar Department of Chemistry, Massachusetts Institute of Technology, Cambridge, Massachusetts 02139-4307, United States
- Diane A. Dickie Department of Chemistry, University of Virginia, Charlottesville, Virginia 22904, United States;
 o orcid.org/0000-0003-0939-3309

Complete contact information is available at: https://pubs.acs.org/10.1021/acs.inorgchem.4c00854

Notes

The authors declare no competing financial interest.

ACKNOWLEDGMENTS

The authors acknowledge the National Science Foundation Chemical Synthesis (CHE-2046544) and Major Research Instrumentation (CHE-2018870) programs for support of this work. R.J.G. acknowledges additional laboratory support through a Beckman Young Investigator Award from the Arnold and Mabel Beckman Foundation. Generous allocation of computing resources from National Computational Infrastructure (NCI), Intersect, and La Trobe University are acknowledged.

REFERENCES

- (1) Su, X.; Bartholome, T. A.; Tidwell, J. R.; Pujol, A.; Yruegas, S.; Martinez, J. J.; Martin, C. D. 9-Borafluorenes: Synthesis, Properties, and Reactivity. *Chem. Rev.* **2021**, *121*, 4147–4192.
- (2) Köster, R.; Benedikt, G. 9-Borafluorenes. Angew. Chem., Int. Ed. 1963, 2, 323–324.
- (3) Braunschweig, H.; Kupfer, T. Recent developments in the chemistry of antiaromatic boroles. *Chem. Commun.* **2011**, *47*, 10903–10914.
- (4) Escande, A.; Ingleson, M. J. Fused polycyclic aromatics incorporating boron in the core: fundamentals and applications. *Chem. Commun.* **2015**, *51*, 6257–6274.
- (5) Barnard, J. H.; Yruegas, S.; Huang, K.; Martin, C. D. Ring expansion reactions of anti-aromatic boroles: a promising synthetic avenue to unsaturated boracycles. *Chem. Commun.* **2016**, *52*, 9985–9901
- (6) Braunschweig, H.; Krummenacher, I.; Wahler, J. Chapter One Free Boroles: The Effect of Antiaromaticity on Their Physical Properties and Chemical Reactivity. In *Advances in Organometallic Chemistry*, Hill, A. F.; Fink, M. J., Eds.; Academic Press: 2013; Vol. 61, pp. 1–53.
- (7) Biswas, S.; Oppel, I. M.; Bettinger, H. F. Synthesis and Structural Characterization of 9-Azido-9-Borafluorene: Monomer and Cyclotrimer of a Borole Azide. *Inorg. Chem.* **2010**, *49*, 4499–4506.
- (8) Müller, M.; Maichle-Mössmer, C.; Bettinger, H. F. BN-Phenanthryne: Cyclotetramerization of an 1,2-Azaborine Derivative. *Angew. Chem., Int. Ed.* **2014**, *53*, 9380–9383.
- (9) Yruegas, S.; Martinez, J. J.; Martin, C. D. Intermolecular insertion reactions of azides into 9-borafluorenes to generate 9,10-B. *N-phenanthrenes. Chem. Commun.* **2018**, 54, 6808–6811.
- (10) Keck, C.; Hahn, J.; Gupta, D.; Bettinger, H. F. Solution Phase Reactivity of Dibenzo[c,e][1,2]azaborinine: Activation and Insertion into Si-E Single Bonds (E = H, OSi(CH3)3, F, Cl) by a BN-Aryne. *Eur. J. Chem.* **2022**, 28, No. e202103614.
- (11) Zhang, W.; Li, G.; Xu, L.; Zhuo, Y.; Wan, W.; Yan, N.; He, G. 9,10-Azaboraphenanthrene-containing small molecules and conju-

- gated polymers: synthesis and their application in chemodosimeters for the ratiometric detection of fluoride ions. *Chem. Sci.* **2018**, *9*, 4444–4450.
- (12) Krebs, J.; Häfner, A.; Fuchs, S.; Guo, X.; Rauch, F.; Eichhorn, A.; Krummenacher, I.; Friedrich, A.; Ji, L.; Finze, M.; Lin, Z.; Braunschweig, H.; Marder, T. B. Backbone-controlled LUMO energy induces intramolecular C—H activation in ortho-bis-9-borafluorene-substituted phenyl and o-carboranyl compounds leading to novel 9,10-diboraanthracene derivatives. *Chem. Sci.* **2022**, *13*, 14165—14178.
- (13) Wang, Z.; Zhou, Y.; Marder, T. B.; Lin, Z. DFT studies on reactions of boroles with carbon monoxide. *Org. Biomol. Chem.* **2017**, 15, 7019–7027.
- (14) Bischof, T.; Beßler, L.; Krummenacher, I.; Erhard, L.; Braunschweig, H.; Finze, M. Construction of a Diverse Range of Boron Heterocycles via Ring Expansion of a Carboranyl-Substituted 9-Borafluorene. *Eur. J. Chem.* **2023**, 29, No. e202300210.
- (15) Lorenz-Rothe, M.; Schellhammer, K. S.; Jägeler-Hoheisel, T.; Meerheim, R.; Kraner, S.; Hein, M. P.; Schünemann, C.; Tietze, M. L.; Hummert, M.; Ortmann, F.; Cuniberti, G.; Körner, C.; Leo, K. From Fluorine to Fluorene—A Route to Thermally Stable aza-BODIPYs for Organic Solar Cell Application. *Adv. Electron. Mater.* 2016, 2, No. 1600152.
- (16) Bluer, K. R.; Laperriere, L. E.; Pujol, A.; Yruegas, S.; Adiraju, V. A. K.; Martin, C. D. Coordination and Ring Expansion of 1,2-Dipolar Molecules with 9-Phenyl-9-borafluorene. *Organometallics* **2018**, *37*, 2917–2927.
- (17) Steffen, A.; Ward, R. M.; Jones, W. D.; Marder, T. B. Dibenzometallacyclopentadienes, boroles and selected transition metal and main group heterocyclopentadienes: Synthesis, catalytic and optical properties. *Coord. Chem. Rev.* **2010**, 254, 1950–1976.
- (18) Rauch, F.; Fuchs, S.; Friedrich, A.; Sieh, D.; Krummenacher, I.; Braunschweig, H.; Finze, M.; Marder, T. B. Highly Stable, Readily Reducible, Fluorescent, Trifluoromethylated 9-Borafluorenes. *Eur. J. Chem.* **2020**, *26*, 12794–12808.
- (19) von Grotthuss, E.; John, A.; Kaese, T.; Wagner, M. Doping Polycyclic Aromatics with Boron for Superior Performance in Materials Science and Catalysis. *Asian J. Org. Chem.* **2018**, *7*, 37–53.
- (20) He, J.; Rauch, F.; Finze, M.; Marder, T. B. (Hetero)arene-fused boroles: a broad spectrum of applications. *Chem. Sci.* **2021**, *12*, 128–147.
- (21) Iida, A.; Sekioka, A.; Yamaguchi, S. Heteroarene-fused boroles: what governs the antiaromaticity and Lewis acidity of the borole skeleton? *Chem. Sci.* **2012**, *3*, 1461–1466.
- (22) Ando, N.; Yamada, T.; Narita, H.; Oehlmann, N. N.; Wagner, M.; Yamaguchi, S. Boron-Doped Polycyclic π -Electron Systems with an Antiaromatic Borole Substructure That Forms Photoresponsive B–P Lewis Adducts. *J. Am. Chem. Soc.* **2021**, *143*, 9944–9951.
- (23) Fukazawa, A.; Yamaguchi, S. Ladder π -Conjugated Materials Containing Main-Group Elements. *Chem.*—Asian J. **2009**, 4, 1386–1400.
- (24) Wakamiya, A.; Mishima, K.; Ekawa, K.; Yamaguchi, S. Kinetically stabilized dibenzoborole as an electron-accepting building unit. *Chem. Commun.* **2008**, 579–581.
- (25) Yamaguchi, S.; Shirasaka, T.; Akiyama, S.; Tamao, K. Dibenzoborole-Containing π -Electron Systems: Remarkable Fluorescence Change Based on the "On/Off" Control of the p π - π * Conjugation. *J. Am. Chem. Soc.* **2002**, *124*, 8816–8817.
- (26) Yamaguchi, S.; Wakamiya, A. Boron as a key component for new π-electron materials. *Pure Appl. Chem.* **2006**, 78, 1413–1424.
- (27) Zhao, Q.; Zhang, H.; Wakamiya, A.; Yamaguchi, S. Coordination-Induced Intramolecular Double Cyclization: Synthesis of Boron-Bridged Dipyridylvinylenes and Dithiazolylvinylenes. *Synthesis* **2009**, 2009, 127–132.
- (28) Urban, M.; Durka, K.; Górka, P.; Wiosna-Sałyga, G.; Nawara, K.; Jankowski, P.; Luliński, S. The effect of locking π -conjugation in organoboron moieties in the structures of luminescent tetracoordinate boron complexes. *Dalton Trans.* **2019**, *48*, 8642–8663.

- (29) Shoji, Y.; Shigeno, N.; Takenouchi, K.; Sugimoto, M.; Fukushima, T. Mechanistic Study of Highly Efficient Direct 1,2-Carboboration of Alkynes with 9-Borafluorenes. *Eur. J. Chem.* **2018**, 24, 13223–13230.
- (30) Berger, C. J.; He, G.; Merten, C.; McDonald, R.; Ferguson, M. J.; Rivard, E. Synthesis and Luminescent Properties of Lewis Base-Appended Borafluorenes. *Inorg. Chem.* **2014**, *53*, 1475–1486.
- (31) Yang, W.; Krantz, K. E.; Dickie, D. A.; Molino, A.; Wilson, D. J. D.; Gilliard, R. J., Jr. Crystalline BP-Doped Phenanthryne via Photolysis of The Elusive Boraphosphaketene. *Angew. Chem., Int. Ed.* **2020**, *59*, 3971–3975.
- (32) Xiang, L.; Wang, J.; Krummenacher, I.; Radacki, K.; Braunschweig, H.; Lin, Z.; Ye, Q. Persistent and Predominantly Localized Boron Radical from the Reduction of a Three-Dimensional Analogue of NHC-Stabilized Borafluorenium. *Eur. J. Chem.* **2023**, *29*, No. e202301270.
- (33) Bonnier, C.; Piers, W. E.; Al-Sheikh Ali, A.; Thompson, A.; Parvez, M. Perfluoroaryl-Substituted Boron Dipyrrinato Complexes. *Organometallics* **2009**, *28*, 4845–4851.
- (34) Zhang, C.; Liu, X.; Wang, J.; Ye, Q. A Three-Dimensional Inorganic Analogue of 9,10-Diazido-9,10-Diboraanthracene A Lewis Superacidic Azido Borane with Reactivity and Stability. *Angew. Chem., Int. Ed.* **2022**, *61*, No. e202205506.
- (35) Zhang, C.; Wang, J.; Lin, Z.; Ye, Q. Synthesis, Characterization, and Properties of Three-Dimensional Analogues of 9-Borafluorenes. *Inorg. Chem.* **2022**, *61*, 18275–18284.
- (36) Zhang, C.; Wang, J.; Su, W.; Lin, Z.; Ye, Q. Synthesis, Characterization, and Density Functional Theory Studies of Three-Dimensional Inorganic Analogues of 9,10-Diboraanthracene—A New Class of Lewis Superacids. *J. Am. Chem. Soc.* 2021, 143, 8552–8558.
- (37) He, J.; Rauch, F.; Krummenacher, I.; Braunschweig, H.; Finze, M.; Marder, T. B. Two derivatives of phenylpyridyl-fused boroles with contrasting electronic properties: decreasing and enhancing the electron accepting ability. *Dalton Trans.* **2021**, *50*, 355–361.
- (38) He, J.; Rauch, F.; Friedrich, A.; Krebs, J.; Krummenacher, I.; Bertermann, R.; Nitsch, J.; Braunschweig, H.; Finze, M.; Marder, T. B. Phenylpyridyl-Fused Boroles: A Unique Coordination Mode and Weak B—N Coordination-Induced Dual Fluorescence. *Angew. Chem., Int. Ed.* **2021**, *60*, 4833–4840.
- (39) Hollister, K. K.; Molino, A.; Breiner, G.; Walley, J. E.; Wentz, K. E.; Conley, A. M.; Dickie, D. A.; Wilson, D. J. D.; Gilliard, R. J. Air-Stable Thermoluminescent Carbodicarbene-Borafluorenium Ions. *J. Am. Chem. Soc.* **2022**, *144*, 590.
- (40) Yang, W.; Krantz, K. E.; Freeman, L. A.; Dickie, D. A.; Molino, A.; Kaur, A.; Wilson, D. J. D.; Gilliard, R. J., Jr. Stable Borepinium and Borafluorenium Heterocycles: A Reversible Thermochromic "Switch" Based on Boron–Oxygen Interactions. *Chem.—Eur. J.* **2019**, 25, 12512–12516.
- (41) Wentz, K. E.; Molino, A.; Weisflog, S. L.; Kaur, A.; Dickie, D. A.; Wilson, D. J. D.; Gilliard, R. J., Jr. Stabilization of the Elusive 9-Carbene-9-Borafluorene Monoanion. *Angew. Chem., Int. Ed.* **2021**, *60*, 13065–13072.
- (42) Wentz, K. E.; Molino, A.; Freeman, L. A.; Dickie, D. A.; Wilson, D. J. D.; Gilliard, R. J., Jr. Reactions of 9-Carbene-9-Borafluorene Monoanion and Selenium: Synthesis of Boryl-Substituted Selenides and Diselenides. *Inorg. Chem.* **2021**, *60*, 13941–13949.
- (43) Wentz, K. E.; Molino, A.; Freeman, L. A.; Dickie, D. A.; Wilson, D. J. D.; Gilliard, R. J., Jr. Activation of Carbon Dioxide by 9-Carbene-9-borafluorene Monoanion: Carbon Monoxide Releasing Transformation of Trioxaborinanone to Luminescent Dioxaborinanone. *J. Am. Chem. Soc.* **2022**, *144*, 16276–16281.
- (44) Wentz, K. E.; Molino, A.; Freeman, L. A.; Dickie, D. A.; Wilson, D. J. D.; Gilliard, R. J., Jr. Systematic Electronic and Structural Studies of 9-Carbene-9-Borafluorene Monoanions and Transformations into Luminescent Boron Spirocycles. *Inorg. Chem.* **2022**, *61*, 17049–17058.
- (45) Wentz, K. E.; Molino, A.; Freeman, L. A.; Dickie, D. A.; Wilson, D. J. D.; Gilliard, R. J., Jr. Approaching Dianionic Tetraoxadiborecine Macrocycles: 10-Membered Bora-Crown Ethers Incorporating

- Borafluorenate Units. Angew. Chem., Int. Ed. 2023, 62, No. e202215772.
- (46) Yang, W.; Krantz, K. E.; Freeman, L. A.; Dickie, D. A.; Molino, A.; Frenking, G.; Pan, S.; Wilson, D. J. D.; Gilliard, R. J., Jr. Persistent Borafluorene Radicals. *Angew. Chem., Int. Ed.* **2020**, *59*, 3850–3854.
- (47) Hollister, K. K.; Wentz, K. E.; Gilliard, R. J., Jr. Redox- and Charge-State Dependent Trends in 5, 6, and 7-Membered Boron Heterocycles: A Neutral Ligand Coordination Chemistry Approach to Boracyclic Cations, Anions, and Radicals. *Acc. Chem. Res.* **2024**, *57*, 1510.
- (48) Tra, B. Y. E.; Molino, A.; Hollister, K. K.; Sarkar, S. K.; Dickie, D. A.; Wilson, D. J. D.; Gilliard, R. J., Jr. Photochemically and Thermally Generated BN-Doped Borafluorenate Heterocycles via Intramolecular Staudinger-Type Reactions. *Inorg. Chem.* **2023**, *62*, 15809–15818.
- (49) Bednarek, C.; Wehl, I.; Jung, N.; Schepers, U.; Bräse, S. The Staudinger Ligation. Chem. Rev. 2020, 120, 4301–4354.
- (50) Melen, R. L.; Lough, A. J.; Stephan, D. W. Boron azides in Staudinger oxidations and cycloadditions. *Dalton Trans.* **2013**, *42*, 8674–8683.
- (51) Courtenay, S.; Walsh, D.; Hawkeswood, S.; Wei, P.; Das, A. K.; Stephan, D. W. Boron and Aluminum Complexes of Sterically Demanding Phosphinimines and Phosphinimides. *Inorg. Chem.* **2007**, 46, 3623–3631.
- (52) Hawkeswood, S.; Wei, P.; Gauld, J. W.; Stephan, D. W. Steric Effects in Metathesis and Reduction Reactions of Phosphinimines with Catechol- and Pinacolboranes. *Inorg. Chem.* **2005**, *44*, 4301–4308.
- (53) Holthausen, M. H.; Mallov, I.; Stephan, D. W. Phosphiniminesubstituted boranes and borenium ions. *Dalton Trans.* **2014**, 43, 15201–15211.
- (54) Chase, P. A.; Henderson, L. D.; Piers, W. E.; Parvez, M.; Clegg, W.; Elsegood, M. R. J. Bifunctional Perfluoroaryl Boranes: Synthesis and Coordination Chemistry with Neutral Lewis Base Donors. *Organometallics* **2006**, *25*, 349–357.
- (55) Chambers, R. D.; Chivers, T. 730. Polyfluoroaryl organometallic compounds. Part II. Pentafluorophenylboron halides and some derived compounds. *Journal of the Chemical Society (Resumed)* 1965, 3933–3939.
- (56) Hübner, A.; Diehl, A. M.; Bolte, M.; Lerner, H.-W.; Wagner, M. High-Temperature Reactivity of the Strongly Electrophilic Pristine 9H-9-Borafluorene. *Organometallics* **2013**, 32, 6827–6833.
- (57) Noguchi, M.; Suzuki, K.; Kobayashi, J.; Yurino, T.; Tsurugi, H.; Mashima, K.; Yamashita, M. Planar and Bent BN-Embedded p-Quinodimethanes Synthesized by Transmetalation of Bis-(trimethylsilyl)-1,4-dihydropyrazines with Chloroborane. *Organometallics* **2018**, *37*, 1833–1836.
- (58) Kluwer, A. M.; Ahmad, I.; Reek, J. N. H. Improved synthesis of monodentate and bidentate 2- and 3-pyridylphosphines. *Tetrahedron Lett.* **2007**, *48*, 2999–3001.
- (59) Drent, E.; Arnoldy, P.; Budzelaar, P. H. M. Homogeneous catalysis by cationic palladium complexes. Precision catalysis in the carbonylation of alkynes. *J. Organomet. Chem.* **1994**, *475*, 57–63.
- (60) Van Overschelde, M.; Vervecken, E.; Modha, S. G.; Cogen, S.; Van der Eycken, E.; Van der Eycken, J. Catalyst-free alcoholysis of phosphane-boranes: a smooth, cheap, and efficient deprotection procedure. *Tetrahedron* **2009**, *65*, 6410–6415.
- (61) Narula, C. K.; Noeth, H. Contribution to the chemistry of boron. 150. Competition between adduct and cation formation in reactions between diorganylborane derivatives and pyridine or lutidines. *Inorg. Chem.* 1985, 24, 2532–2539.
- (62) Hübner, A.; Qu, Z.-W.; Englert, U.; Bolte, M.; Lerner, H.-W.; Holthausen, M. C.; Wagner, M. Main-Chain Boron-Containing Oligophenylenes via Ring-Opening Polymerization of 9-H-9-Borafluorene. *J. Am. Chem. Soc.* **2011**, *133*, 4596–4609.
- (63) Tra, B. Y. E.; Molino, A.; Hollister, K. K.; Sarkar, S. K.; Dickie, D. A.; Wilson, D. J. D.; Gilliard, R. J., Jr. Photochemically- and Thermally-Generated BN- and BNP-Doped Borafluorenate Hetero-

- cycles via Intramolecular Staudinger-Type Reactions. ChemRxiv 2023, 62, 15809.
- (64) Pyykkö, P.; Atsumi, M. Molecular Double-Bond Covalent Radii for Elements Li–E112. Eur. J. Chem. 2009, 15, 12770–12779.
- (65) Pyykkö, P. Additive Covalent Radii for Single-, Double-, and Triple-Bonded Molecules and Tetrahedrally Bonded Crystals: A Summary. *J. Phys. Chem. A* **2015**, *119*, 2326–2337.
- (66) Keck, C.; Hahn, J.; Gupta, D.; Bettinger, H. F. Solution Phase Reactivity of Dibenzo[c,e][1,2]azaborinine: Activation and Insertion into Si-E Single Bonds (E = H, OSi(CH3)3, F, Cl) by a BN-Aryne. *Eur. J. Chem.* **2022**, 28, No. e202103614.
- (67) Neese, F. Software update: The ORCA program system—Version 5.0. WIREs Comput. Mol. Sci. 2022, 12, No. e1606.
- (68) Perdew, J. P.; Ernzerhof, M.; Burke, K. Rationale for mixing exact exchange with density functional approximations. *J. Chem. Phys.* **1996**, *105*, 9982–9985.
- (69) Adamo, C.; Barone, V. Toward reliable density functional methods without adjustable parameters: The PBE0 model. *J. Chem. Phys.* **1999**, *110*, 6158–6170.
- (70) Grimme, S.; Antony, J.; Ehrlich, S.; Krieg, H. A consistent and accurate ab initio parametrization of density functional dispersion correction (DFT-D) for the 94 elements H-Pu. *J. Chem. Phys.* **2010**, 132, No. 154104.
- (71) Grimme, S.; Ehrlich, S.; Goerigk, L. Effect of the damping function in dispersion corrected density functional theory. *J. Comput. Chem.* **2011**, 32, 1456–1465.
- (72) Weigend, F.; Ahlrichs, R. Balanced basis sets of split valence, triple zeta valence and quadruple zeta valence quality for H to Rn: Design and assessment of accuracy. *Phys. Chem. Chem. Phys.* **2005**, 7, 3297–3305.
- (73) Barone, V.; Cossi, M. Quantum Calculation of Molecular Energies and Energy Gradients in Solution by a Conductor Solvent Model. *J. Phys. Chem. A* **1998**, *102*, 1995–2001.
- (74) Neese, F.; Wennmohs, F.; Hansen, A.; Becker, U. Efficient, approximate and parallel Hartree—Fock and hybrid DFT calculations. A 'chain-of-spheres' algorithm for the Hartree—Fock exchange. *Chem. Phys.* **2009**, *356*, 98–109.
- (75) Asgeirsson, V.; Birgisson, B. O.; Bjornsson, R.; Becker, U.; Neese, F.; Riplinger, C.; Jónsson, H. Nudged Elastic Band Method for Molecular Reactions Using Energy-Weighted Springs Combined with Eigenvector Following. *J. Chem. Theory Comput* **2021**, *17*, 4929–4945.